INSTITUTE OF PHYSICS PUBLISHING JOURNAL OF OPTICS A: PURE AND APPLIED OPTICS

J. Opt. A: Pure Appl. Opt. **8** (2006) 244–251 doi:10.1088/1464-4258/8/3/004

Fresnel diffraction and polychromatic effects on angle-of-arrival fluctuations

Amokrane Berdja[1,2], **Julien Borgnino**[2] **and Abdenour Irbah**[3]

[1] Centre de Recherche en Astronomie Astrophysique et Géophysique, BP 63, Route de l'Observatoire, 16340 Bouzaréah, Alger, Algeria
[2] Laboratoire Universitaire d'Astrophysique de Nice UMR 6525, Université de Nice-Sophia Antipolis, Parc Valrose F-06108 Nice Cedex 2, France
[3] Service d'Aéronomie, CNRS, BP 63, 91371 Verrières le Buisson Cedex, France

E-mail: berdja@unice.fr, borgnino@unice.fr and irbah@aerov.jussieu.fr

Received 22 June 2005, accepted for publication 3 January 2006
Published 24 January 2006
Online at stacks.iop.org/JOptA/8/244

Abstract
Seeing monitoring in astronomy is widely based on the statistical analysis of angle-of-arrival (AA) fluctuations, which are usually modelled in the framework of the near-field approximation where diffraction through turbulence is ignored. They are consequently believed to be completely independent of wavelength. We discuss in this paper the influence of Fresnel diffraction from distant turbulence layers on multi-wavelength (polychromatic) AA fluctuations. For this purpose we propose a model for polychromatic AA fluctuations in weak turbulence conditions and derive an analytical model for their variance in the case where scintillation is ignored. We also present a numerical simulation that includes scintillation and justifies that this latter may be neglected in the analytical model.

Keywords: turbulence, atmospheric effects, high angular resolution, angle of arrival, seeing monitor

1. Introduction

For a long time now, turbulence has been well recognized as one of the major limitations to the quality of ground-based astronomical imaging [2–4]. Turbulence causes heterogeneous and time-changing refractive index fluctuations in the atmosphere and while propagating through, light waves from outer space undergo phase and amplitude perturbations [1]. Optical turbulence causes the astronomical images to be severely damaged [4] even if its effects can be more or less overcome today with some special observing techniques based on speckle interferometry [4, 9] and adaptive optics [7, 8]. It remains necessary however to have pertinent information on the optical turbulence effects (like image motion) [5] with the so-called seeing monitors.

Some seeing monitors like DIMM [10–12] and GSM [13, 14] are based on statistical analyses of angle-of-arrival (AA) fluctuations [15–17, 12]. The AA fluctuations are the local turbulence-induced angular deviations of light from its initial direction of incidence. They are responsible for the apparent motion of the astronomical output images whenever seen with a telescope. Image motion is shown [1] to be proportional to the normalized averaging of the AA fluctuations all over an entrance pupil where they are weighted by the instantaneous intensity fluctuations resulting from scintillation. In all the following we will focus on these AA fluctuations at any given position on the entrance pupil of a telescope by looking into them as local contributors to turbulence-induced image motion.

Phase and amplitude fluctuations are known to depend upon wavelength [23] and they have been investigated from the polychromatic point of view [22, 24, 27]. The influence of scintillation on image motion has been also investigated [21, 25, 26] but we do not know actually if polychromatic AA fluctuations, or at least a clear justification of using the near-field approximation for them, have ever been discussed. It should be noted however that the diffraction effect on the pupil-related Zernike tilt (Z-tilt) [4] has been described in the monochromatic case [20]. We are investigating here the general case of polychromatic AA fluctuations without any entrance pupil effect. One may consider that Z-tilt is sufficiently equivalent to image motion (G-tilt) to be considered as a good approximation of the object of our study. However, Z-tilt in the most general case does participate

 © 2006 IOP Publishing Ltd Printed in the UK

partially (together with other non-symmetrical Zernike modes) to image motion. A closer look (see for example [17]) shows also that Z-tilt and G-tilt are dissimilar with different spectra. They are thus differently influenced by diffraction. As stated before, we focus here on the local pupil-independent contributions to image motion, i.e., the AA fluctuations.

In the following we will briefly review the near-field approximation and its implications on the modelling of the AA fluctuations and then introduce diffraction in the polychromatic case.

2. Diffraction and the near-field approximation

Let $\varphi_0(\lambda, \vec{r})$ be the instantaneous turbulence-induced phase fluctuations of a monochromatic light wave at the entrance pupil. It depends upon wavelength λ and upon the two-dimensional position $\vec{r}$ on the pupil. We do not care anywhere in this paper about the temporal evolution of the optical turbulence.

The monochromatic AA fluctuations $\vec{\alpha}(\lambda, \vec{r})$, defined as the local fluctuations of the normal at each point to the perturbed wavefront, are given by [1, 2]

$$\vec{\alpha}(\lambda, \vec{r}) = \frac{-\lambda}{2\pi} \vec{\nabla} \varphi_0(\lambda, \vec{r}) \tag{1}$$

where $\vec{\nabla}$ denotes a two-dimensional spatial gradient.

We first recall the most basic results of the optical turbulence theory as formulated for astronomical observation. We consider for this purpose a single turbulent layer situated at an altitude h above the telescope. All results can easily be generalized afterwards to multi-layered turbulence.

The light's complex amplitude perturbations $\psi(\lambda, \vec{r})$ as expressed by phase and log-amplitude fluctuations (which are respectively denoted by $\varphi(\lambda, \vec{r})$ and $\chi(\lambda, \vec{r})$) are written [3] in the following manner:

$$\psi(\lambda, \vec{r}) = \exp\{\chi(\lambda, \vec{r}) + \mathrm{i}\varphi(\lambda, \vec{r})\}. \tag{2}$$

In the thin-screen model [2], light propagation through the turbulence layer undergoes only phase fluctuations. The output phase fluctuations $\varphi_h(\lambda, \vec{r})$ at the altitude h are related to refractive index fluctuations $n(\lambda, \vec{r}, h)$ along the propagation path:

$$\varphi_h(\lambda, \vec{r}) = \frac{2\pi}{\lambda} \int_h^{h+\delta h} \mathrm{d}h' n(\lambda, \vec{r}, h') \tag{3}$$

where δh denotes the layer thickness.

Light propagation from the layer output to the telescope pupil is correctly described by Fresnel diffraction [2]. It is important to note here that diffraction influences complex amplitude, i.e., both phase and log-amplitude. At ground level, phase and log-amplitude fluctuations are given by [2, 6]

$$\varphi_0(\lambda, \vec{r}) = \varphi_h(\lambda, \vec{r}) \otimes \frac{\sin\{\pi r^2/\lambda h\}}{\lambda h} \tag{4}$$

$$\chi_0(\lambda, \vec{r}) = \varphi_h(\lambda, \vec{r}) \otimes \frac{\cos\{\pi r^2/\lambda h\}}{\lambda h} \tag{5}$$

where $\otimes$ denotes a two-dimensional spatial convolution product.

This result corresponds to the first-order Rytov solution of the corresponding wave propagation equation in the weak turbulence regime [4].

In describing long-exposure images within the framework of this model, it is clearly shown that blurring does not depend upon diffraction [2]. Indeed, long-exposure image blurring is related to the spatial covariance (second-order moment) of light's complex amplitude perturbations, which is invariant under Fresnel diffraction [2]. It is equivalent to having the whole turbulence situated at the telescope level, inducing only phase fluctuations. It is what is called the near-field approximation. What needs to be kept in mind is that long-exposure image blurring does not depend upon diffraction although phase and log-amplitude fluctuations do depend upon it. In other respects, the independence to diffraction of long-exposure image blurring does not mean at all that phase and log-amplitude do not depend upon diffraction.

The near-field approximation has been extended to phase fluctuations and thus to AA fluctuations. Diffraction is still in use however in describing log-amplitude fluctuations, which give rise to scintillation [19, 18]. Let us review now the incidence of the near-field approximation on AA fluctuations. We can easily see from equations (1) and (3) that AA fluctuations do not depend upon wavelength if we ignore the diffraction term which corresponds to the second factor in the convolution product of equation (4). We must also assume here that the refractive index fluctuations do not depend upon wavelength. It results that AA fluctuations are achromatic and are the same at any wavelength in the near-field approximation [12]. Assuming this, seeing monitors based on AA fluctuations have no spectral filters [12] in order to exploit maximum light flux on receptors. This achromatic approach of AA fluctuations allows also ignoring such considerations as stellar spectra and detector responses, leading to simpler treatments.

It is then justified to wonder whether the near-field approximation is sufficient to describe AA fluctuations correctly. We must also note that diffraction is expected to make AA fluctuations at different wavelengths somehow different from one another and more or less uncorrelated. For these reasons, we attempt in the following to model polychromatic (multi-wavelength) AA fluctuations by taking into account diffraction.

3. A model for polychromatic AA fluctuations

AA fluctuations are responsible for image motion in the telescope focal plane. Stellar image motion is obtained by the instantaneous centroid position. In this context, the stellar image position with polychromatic light is given by instantaneous intensity-related averaging of its different monochromatic contributors. We will thus consider the same formalism for polychromatic AA fluctuations. We must also suppose that the monochromatic components at different wavelengths are optically incoherent and that their combination is accurately expressed by carrying a summation through intensities without including interference. This is reasonably achieved with polychromatic bandwidths $\Delta\lambda$ far larger than individual atomic spectral emission-peak bandwidths.

In this manner, polychromatic AA fluctuations $\vec{\alpha}(\vec{r})$ can be seen as an average of their monochromatic contributors $\vec{\alpha}(\lambda, \vec{r})$ weighted by the intensity. The intensity is also partly affected by the instrument response and scintillation due to atmospheric turbulence. We can therefore write

$$\vec{\alpha}(\vec{r}) = \frac{\int_{\lambda_0-\Delta\lambda/2}^{\lambda_0+\Delta\lambda/2} \mathrm{d}\lambda\ \rho(\lambda)\exp\{2\chi_0(\lambda)+2\chi(\lambda,\vec{r})\}\vec{\alpha}(\lambda,\vec{r})}{\int_{\lambda_0-\Delta\lambda/2}^{\lambda_0+\Delta\lambda/2} \mathrm{d}\lambda\ \rho(\lambda)\exp\{2\chi_0(\lambda)+2\chi(\lambda,\vec{r})\}}. \tag{6}$$

$\chi_0(\lambda)$ is the non-perturbed log-amplitude, which is related to the stellar spectrum as transmitted through the atmosphere. $\chi(\lambda, \vec{r})$ is the turbulence-induced log-amplitude perturbation, which is responsible for scintillation. $\rho(\lambda)$ is a term describing the instrument intensity response.

In order to characterize the level of the polychromatic effect importance we will consider in our case a finite bandwidth $\Delta\lambda$ around a given central wavelength λ_0. AA fluctuations in both achromatic and polychromatic approaches must be compared via their statistical properties because they are random quantities. We will limit ourselves to comparing their statistical variances.

4. Polychromatic AA fluctuations ignoring scintillation

If scintillation has to be ignored as a first approximation then we put $\chi(\lambda, \vec{r}) = 0$ in equation (6):

$$\vec{\alpha}(\vec{r}) = \frac{\int_{\lambda_a}^{\lambda_b} \mathrm{d}\lambda\ F(\lambda)\vec{\alpha}(\lambda,\vec{r})}{\int_{\lambda_a}^{\lambda_b} \mathrm{d}\lambda\ F(\lambda)} \tag{7}$$

where $F(\lambda) = \rho(\lambda)\exp\{2\chi_0(\lambda)\}$, $\lambda_a = \lambda_0 - \Delta\lambda/2$ and $\lambda_b = \lambda_0 + \Delta\lambda/2$.

As in real-life measurements, we just consider one component α of the AA fluctuations along a given direction such as $\alpha = \vec{\alpha}\vec{i}$ with $\vec{r} = x\vec{i} + y\vec{j}$. This does not in any case limit this study.

The statistical variance σ_α^2 of the polychromatic AA fluctuations α is given by

$$\sigma_\alpha^2 = \frac{\int_{\lambda_a}^{\lambda_b} \mathrm{d}\lambda_1 \int_{\lambda_a}^{\lambda_b} \mathrm{d}\lambda_2 F(\lambda_1)F(\lambda_2)\langle\alpha(\lambda_1,\vec{r})\alpha^*(\lambda_2,\vec{r})\rangle}{\int_{\lambda_a}^{\lambda_b} \mathrm{d}\lambda_1 \int_{\lambda_a}^{\lambda_b} \mathrm{d}\lambda_2 F(\lambda_1)F(\lambda_2)} \tag{8}$$

where $\langle\ \rangle$ denotes ensemble averaging.

The statistical averaging that appears in equation (8) can be labelled the chromatic covariance for the wavelengths λ_1 and λ_2 (specifically at these wavelengths). It is expressed by

$$B_\alpha([\lambda_1,\lambda_2],\vec{0}) = \langle\alpha(\lambda_1,\vec{r})\alpha^*(\lambda_2,\vec{r})\rangle. \tag{9}$$

We recall that we are considering a single turbulence layer situated at an altitude h giving rise to AA fluctuations at the telescope entrance pupil.

Let us now denote $\tilde{\varphi}_h(\lambda, \vec{f})$, the two-dimensional spatial Fourier transform of $\varphi_h(\lambda, \vec{r})$:

$$\varphi_h(\lambda,\vec{r}) = \int \mathrm{d}\vec{f}\,\tilde{\varphi}_h(\lambda,\vec{f})\exp\{2\pi\mathrm{i}\vec{f}\vec{r}\} = \mathrm{FT}^{-1}\{\tilde{\varphi}_h(\lambda,\vec{f})\}; \tag{10}$$

$\vec{f}$ is the two-dimensional spatial frequency with $\vec{f} = f_x\vec{i} + f_y\vec{j}$ and $\mathrm{FT}^{-1}\{\ \}$ denotes the inverse spatial Fourier transform.

Using equations (1) and (4), the monochromatic AA fluctuations are given by

$$\alpha(\lambda,\vec{r}) = \frac{-\lambda}{2\pi}\mathrm{FT}^{-1}\{2\pi\mathrm{i}f_x\tilde{\varphi}_h(\lambda,\vec{f})\cos\{\pi\lambda h f^2\}\}. \tag{11}$$

The chromatic covariance can then be written as

$$B_\alpha([\lambda_1,\lambda_2],\vec{0}) = \lambda_1\lambda_2\int \mathrm{d}\vec{f}_1\int \mathrm{d}\vec{f}_2 f_{1x}f_{2x} \times \cos\{\pi\lambda_1 h f_1^2\}\cos\{\pi\lambda_2 h f_2^2\}\langle\tilde{\varphi}_h(\lambda_1,\vec{f}_1)\tilde{\varphi}_h^*(\lambda_2,\vec{f}_2)\rangle. \tag{12}$$

The statistical term $\langle\tilde{\varphi}_h(\lambda_1,\vec{f}_1)\tilde{\varphi}_h^*(\lambda_2,\vec{f}_2)\rangle$ occurs in the framework of the near-field approximation, i.e., no diffraction at the layer output. We obtain thus after simple operations

$$\langle\tilde{\varphi}_h(\lambda_1,\vec{f}_1)\tilde{\varphi}_h^*(\lambda_2,\vec{f}_2)\rangle = \int \mathrm{d}\vec{r}_1\exp\{-2\pi\mathrm{i}[\vec{f}_1-\vec{f}_2]\vec{r}_1\} \times \int \mathrm{d}\vec{\rho}\langle\varphi_h(\lambda_1,\vec{r}_1)\varphi_h(\lambda_2,\vec{r}_1-\vec{\rho})\rangle\exp\{-2\pi\mathrm{i}\vec{f}_2\vec{\rho}\}. \tag{13}$$

Here appears the spatial-and-chromatic covariance of phase fluctuations in the near-field approximation. This quantity has been already described [22, 24] and we will express it in a different shape:

$$\langle\tilde{\varphi}_h^*(\lambda_1,\vec{f}_1)\tilde{\varphi}_h(\lambda_2,\vec{f}_2)\rangle = W_{\varphi_h}^{\mathrm{nf}}([\lambda_1,\lambda_2],\vec{f}_2)\delta\{\vec{f}_2-\vec{f}_1\}; \tag{14}$$

nf denotes the use of the near-field approximation and δ denotes the Dirac function.

For example, in the case where the optical turbulence obeys the Von Kàrmàn and Hill-Andrews models [31] then we can write

$$W_{\varphi_h}^{\mathrm{nf}}([\lambda_1,\lambda_2],\vec{f}) = 0.3827\frac{\sqrt{C_n^2(\lambda_1)C_n^2(\lambda_2)}\delta h}{\lambda_1\lambda_2} \times [f^2+L_0^{-2}]^{-11/6}[1+3.4310fl_0-0.5384[fl_0]^{7/6}] \times \exp\left\{-\left[\frac{2\pi f l_0}{3.3}\right]^2\right\} \tag{15}$$

where $C_n^2(\lambda)$ is the constant structure for refractive index fluctuations. L_0 and l_0 are respectively the outer and inner scales of the optical turbulence.

Because the refractive index depends intrinsically upon wavelength, it is natural that the constant structure $C_n^2(\lambda)$ depends upon wavelength too. Although it is important, we will not discuss this topic in this paper, which is restricted to the diffraction effects.

We also suppose here that l_0 and L_0 do not depend upon wavelength, allowing us to write $W_{\varphi_h}^{\mathrm{nf}}([\lambda_1,\lambda_2],\vec{f})$ in this simplified form:

$$W_{\varphi_h}^{\mathrm{nf}}([\lambda_1,\lambda_2],\vec{f}) = \frac{\sqrt{C_n^2(\lambda_1)C_n^2(\lambda_2)}\delta h}{\lambda_1\lambda_2}G_{\varphi_h}^{\mathrm{nf}}(\vec{f}). \tag{16}$$

$G_{\varphi_h}^{\mathrm{nf}}(\vec{f})$ is the part of $W_{\varphi_h}^{\mathrm{nf}}([\lambda_1,\lambda_2],\vec{f})$ that does not depend upon wavelength and this writing can apply to different optical turbulence models [28–30].

We then obtain

$$B_\alpha([\lambda_1,\lambda_2],\vec{0}) = \sqrt{C_n^2(\lambda_1)C_n^2(\lambda_2)}\delta h\int \mathrm{d}\vec{f}\,f_x^2 \times \cos\{\pi\lambda_1 h f^2\}\cos\{\pi\lambda_2 h f^2\}G_{\varphi_h}^{\mathrm{nf}}(\vec{f}). \tag{17}$$

The variance becomes

$$\sigma_\alpha^2 = \frac{\int \mathrm{d}\vec{f}\, G_{\varphi_h}^{\mathrm{nf}}(\vec{f}) f_x^2 [\int_{\lambda_a}^{\lambda_b} \mathrm{d}\lambda F(\lambda)\sqrt{C_n^2(\lambda)}\cos\{\pi\lambda h f^2\}]^2 \delta h}{[\int_{\lambda_a}^{\lambda_b} \mathrm{d}\lambda F(\lambda)]^2}. \tag{18}$$

Since $G_{\varphi_h}^{\mathrm{nf}}(\vec{f})$ is isotropic with respect to the spatial frequency $\vec{f}$, we finally obtain

$$\sigma_\alpha^2 = \left\{\pi \int_0^\infty \mathrm{d}f\, G_{\varphi_h}^{\mathrm{nf}}(f) f^3 \left[\int_{\lambda_a}^{\lambda_b} \mathrm{d}\lambda F(\lambda)\sqrt{C_n^2(\lambda)} \times \cos\{\pi\lambda h f^2\}\right]^2 \delta h\right\}\left[\int_{\lambda_a}^{\lambda_b} \mathrm{d}\lambda F(\lambda)\right]^{-2}. \tag{19}$$

This result can also be generalized to the case where l_0 and L_0 have wavelength dependences.

4.1. Results

Diffraction effects on AA fluctuations in both monochromatic and polychromatic cases can be studied using equation (19). This is easily done by giving constant values to $F(\lambda)$ and $C_n^2(\lambda)\delta h$. We recall that we are still always ignoring scintillation.

In this case we will have

$$\sigma_\alpha^2 \propto \frac{\pi \int_0^\infty \mathrm{d}f\, G_{\varphi_h}^{\mathrm{nf}}(f) f^3 [\int_{\lambda_a}^{\lambda_b} \mathrm{d}\lambda \cos\{\pi\lambda h f^2\}]^2}{[\int_{\lambda_a}^{\lambda_b} \mathrm{d}\lambda]^2} \tag{20}$$

where $\propto$ denotes proportionality.

The variance is numerically integrated according to equation (20) for different values of altitude h and wavelength bandwidth $\Delta\lambda$.

We will quantify the diffraction effect magnitude for a given altitude h and wavelength band $[\lambda_0, \Delta\lambda]$ by defining the 'normalized difference' ND $(\lambda_0, \Delta\lambda, h)$ as follows:

$$\mathrm{ND}(\lambda_0, \Delta\lambda, h) = \frac{\sigma_\alpha^2(\lambda_0, \Delta\lambda, h) - \sigma_\alpha^2(\lambda_0, 0, 0)}{\sigma_\alpha^2(\lambda_0, 0, 0)}. \tag{21}$$

This quantity expresses the difference between the variance of AA fluctuations when diffraction is taken into account in theoretical models and when it is not. It is normalized with the variance of AA fluctuations when diffraction is ignored.

Because of the achromatism of the AA fluctuations in the near-field approximation, $\sigma_\alpha^2(\lambda_0, \Delta\lambda, 0)$ is equal to $\sigma_\alpha^2(\lambda_0, 0, 0)$.

4.2. Effect of diffraction on monochromatic AA fluctuations

Figure 1 shows the 'normalized difference' behaviour with altitude for some wavelengths in the monochromatic case, obtained by putting $\Delta\lambda = 0$ in equations (20) and (21). It is clearly observed that diffraction effects are far from being negligible for AA fluctuations. As can be seen in figure 1, the error is sufficiently important to question seriously the validity of the near-field approximation to describe AA fluctuation statistics.

We suppose indeed within the framework of the near-field approximation that AA fluctuations measured at ground level ($h = 0$) are the same as those arising from the turbulent layer ($h \neq 0$) but in fact these latter have greater variance. AA fluctuations at the layer's output level correspond to ground-based image blurring since this latter is not affected by diffraction. Neglecting diffraction leads to an overestimating of the astronomical imaging quality if deduced from ground AA fluctuation statistics. This point will be discussed in more detail in section 5.

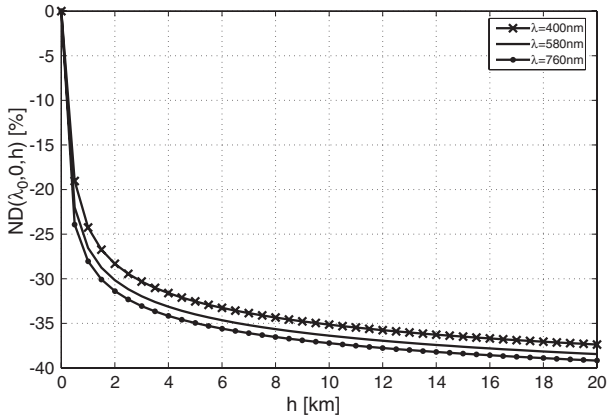


Figure 1. 'Normalized difference' behaviour with altitude in the monochromatic case according to equations (20) and (21). In this case L_0 and l_0 are taken respectively equal to 30 and 0.01 m. Samplings for numerical integrations are $\delta\lambda = 0.1$ nm and $\delta f = 0.005\ \mathrm{m}^{-1}$.

We can notice here that variance is somehow more sensitive to altitude than to wavelength. We must however keep in mind that even if their variances are close one to the other, the instantaneous AA fluctuations at different wavelengths can be more or less uncorrelated. That is what is to be shown in the polychromatic case.

4.3. Effect of diffraction on polychromatic AA fluctuations

The 'normalized difference' versus altitude h, computed in the polychromatic case for a fixed central wavelength λ_0 and for different values of wavelength bandwidth $\Delta\lambda$, is displayed in figure 2. It is observed that measuring AA fluctuations on a wide wavelength bandwidth has a strong additive effect on the departure of their variance from the case where diffraction is ignored. This is due to the uncorrelated monochromatic AA fluctuations at different wavelengths when affected by diffraction.

We show here that the near-field approximation is not systematically justified in describing the AA fluctuation statistics and that both diffraction (altitude) and the polychromatic effects have to be taken into account. We do not make any statement about the turbulence height since this latter is supposed to be unknown and variable.

In the next section we will see an example of how the importance of diffraction in AA fluctuations can influence a concrete situation. We have chosen to look at seeing monitoring with DIMM.

5. Application to a seeing monitor: the DIMM case

A differential image motion monitor (DIMM) measures the difference between the instantaneous positions of the two

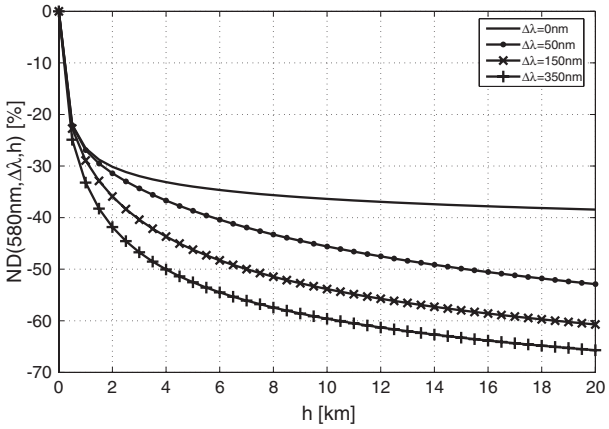


Figure 2. 'Normalized difference' behaviour with altitude in the polychromatic case according to equations (20) and (21). In this case $L_0 = 30$ m, $l_0 = 0.01$ m and $\lambda_0 = 580$ nm. Samplings for numerical integrations are $\delta\lambda = 0.1$ nm and $\delta f = 0.005$ m^{-1}.

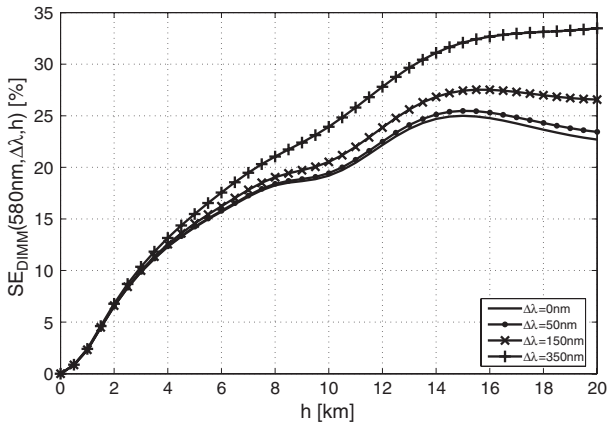


Figure 3. Plot of the 'systematic error' on the Fried parameter r_0 with respect to altitude according to equations (23) and (25). In this case $D = 4$ cm, $B = 20$ cm, $\gamma = 0$ (longitudinal differential image motion), $L_0 = 30$ m, $l_0 = 0.01$ m and $\lambda_0 = 580$ nm. Samplings for numerical integrations are $\delta\lambda = 0.1$ nm and $\delta f = 0.005$ m^{-1}.

images of a single star in its telescope focal plane. The dual image is obtained through two sub-apertures on the pupil plane [10]. Image motion is due to the averaging of AA fluctuations over each sub-aperture. A spatial frequency filtering occurs on AA fluctuations when averaged over the circular sub-apertures of diameter D and when the differential operation over the baseline $\vec{B}$ is done.

The DIMM filtering function DIMM $(\vec{f})$ is given by [12, 16]

$$\mathrm{DIMM}(\vec{f}) = 2\left[\frac{2J_1\{\pi Df\}}{\pi Df}\right]^2 [1 - J_0\{2\pi fB\} + \cos\{2\gamma\}J_2\{2\pi fB\}] \tag{22}$$

where γ is the angle between the baseline and image motion's orientation with $\vec{B}\vec{i} = B\cos\{\gamma\}$. $J_n\{\,\}$ is the Bessel function of the first kind and nth order.

Differential image motion in a DIMM is usually computed in two particular configurations that are longitudinal and transversal, corresponding respectively to $\gamma = 0$ and $\pi/2$.

As was done to obtain equation (20), we attribute constant values to $F(\lambda)$ and $C_n^2(\lambda)\delta h$. The variance of the polychromatic differential image motion σ^2_{DIM} is then written as

$$\sigma^2_{\mathrm{DIM}} \propto \left\{\pi \int_0^\infty \mathrm{d}f G^{\mathrm{nf}}_{\varphi_h}(f) f^3 \left[\int_{\lambda_a}^{\lambda_b} \mathrm{d}\lambda \times \cos\{\pi\lambda h f^2\}\right]^2 \mathrm{DIMM}(\vec{f})\right\} \left\{\left[\int_{\lambda_a}^{\lambda_b} \mathrm{d}\lambda\right]^2\right\}^{-1}. \tag{23}$$

The astronomical imaging quality is usually characterized by the Fried parameter $r_0(\lambda_0)$ that relates to the long-exposure image width of an unresolved star [4]. Fried's parameter is estimated using the DIMM from the variance of the differential image motion [10]. We will use the following expression in which analytical development is based on the near-field approximation:

$$r_0(\lambda_0) = [\sigma^2_{\mathrm{DIM}}/[2\lambda_0^2[0.179D^{-1/3} - 0.145B^{-1/3} \times [1 - \cos^2\{\gamma\}/3]]]]^{-3/5}. \tag{24}$$

Let us first suppose that a variance of differential image motion σ^2_{DIM} corresponding to an unknown altitude h of a single layer turbulence has been measured at ground level.

Assuming the validity of the near-field approximation, we estimate $r_0^{\mathrm{DIMM}}(\lambda_0)$ from σ^2_{DIM} with equation (24) where σ^2_{DIM} is in an unknown manner affected by diffraction and is computed using equation (4) in a case where $h \neq 0$. It is the Fried parameter obtained with a model that ignores diffraction and polychromatic effects.

One has rather to measure $r_0^{\mathrm{real}}(\lambda_0, \Delta\lambda, h)$ that really characterizes the astronomical imaging quality on the ground. In this case we compute σ^2_{DIM} using equation (23) with $h = 0$ and then estimate $r_0^{\mathrm{real}}(\lambda_0, \Delta\lambda, h)$ using equation (24). This is equivalent to considering the DIMM situated at the turbulence layer's output where equation (24) is valid.

We define a systematic error $\mathrm{SE}_{\mathrm{DIMM}}(\lambda_0, \Delta\lambda, h)$ that results from supposing the validity of the near-field approximation in estimating the Fried parameter with a DIMM. This systematic error is written as the following:

$$\mathrm{SE}_{\mathrm{DIMM}}(\lambda_0, \Delta\lambda, h) = \frac{r_0^{\mathrm{DIMM}}(\lambda_0) - r_0^{\mathrm{real}}(\lambda_0, \Delta\lambda, h)}{r_0^{\mathrm{real}}(\lambda_0, \Delta\lambda, h)}. \tag{25}$$

This quantity expresses the relative departure of the estimated Fried parameter $r_0^{\mathrm{DIMM}}(\lambda_0)$ when ignoring diffraction and polychromatic effects from the Fried parameter $r_0^{\mathrm{real}}(\lambda_0, \Delta\lambda, h)$ that really defines the astronomical imaging quality.

The systematic error on $r_0(\lambda_0)$ estimations versus altitudes h is computed from a numerical integration of equation (23) in the case of a typical DIMM. Results are presented in figures 3 and 4 where longitudinal ($\gamma = 0$) and transversal ($\gamma = \pi/2$) differential image motion are respectively considered. They reveal that diffraction and polychromatic effects are still important and far from being negligible. It is probably significant to notice that this error is more important in the case of transversal differential image motion (figure 4) than in the case of longitudinal differential image motion (figure 3).

When measuring differential image motion at ground level one usually supposes that turbulence is localized close to the

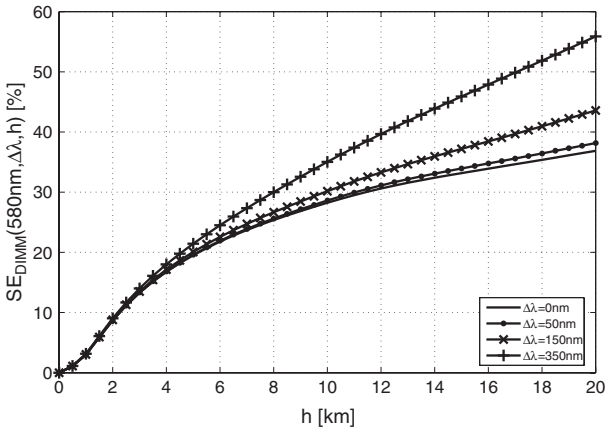


Figure 4. Plot of the 'systematic error' on the Fried parameter r_0 with respect to altitude according to equations (23) and (25). In this case $D = 4$ cm, $B = 20$ cm, $\gamma = \pi/2$ (transversal differential image motion), $L_0 = 30$ m, $l_0 = 0.01$ m and $\lambda_0 = 580$ nm. Samplings for numerical integrations are $\delta\lambda = 0.1$ nm and $\delta f = 0.005$ m^{-1}.

ground. In this specific situation the near-field approximation is justified and using equation (24) for example should give the Fried parameter that characterizes the astronomical imaging quality. However, for the optical turbulence arising from altitude $h \neq 0$, the differential image motion at ground level is affected by diffraction and polychromatic effects and has lower variance than differential image motion originating at the turbulence layer output. We have a situation where the astronomical imaging quality may appear unaltered by diffraction so that the Fried parameter has the same value at the turbulence layer output and at ground level. On the other hand the differential image motion is weakened by diffraction and polychromatic effects as if originating from weaker turbulence. It is then clear that the lower variance differential image motion will give a greater Fried parameter if one ignores diffraction and polychromatic effects. The Fried parameter and correlatively the astronomical imaging quality are clearly overestimated. This discussion does not reduce to DIMM but extends also to seeing monitoring using image motion in general. DIMM here is only a demonstrative example.

In order to minimize the polychromatic effect one can think to use wavelength filtering. A narrow wavelength filtering reduces the light flux and increases photonic noises. An optimal compromise between the systematic error due to the polychromatic effects and the dispersive error due to the photonic noises has thus to be found. Such a discussion requires more technical considerations but a filtering resolves the problem only moderately. One can see indeed from figures 3 and 4 that even with monochromatic light the diffraction effect is still non-negligible.

The solution in our opinion is simply to take into account diffraction and polychromatic effects in the models describing differential image motion, for example versus the optical turbulence parameters as we have done in equation (23).

It should be emphasized that applying a model that takes into account diffraction and polychromatic effects requires the knowledge of the turbulence distribution along altitude, or at least an estimate of the altitude of a single layer equivalent to the whole turbulent terrestrial atmosphere. This is not actually possible with DIMM as far as we know, but such a model has to be useful to seeing monitors based on image motion measurement that also have the capability to estimate the turbulence altitude. The model we propose is a theoretical framework for interpreting observations with such instruments.

6. Polychromatic AA fluctuations without ignoring scintillation

A numerical simulation is performed in order to look into the contribution of scintillation to polychromatic AA fluctuations.

6.1. Simulation method

The purpose of the simulation is to obtain quasi-random samples (realizations) of AA fluctuation series with convenient statistical properties. To do so, we must generate simultaneous monochromatic log-amplitude fluctuations $\chi(\lambda, \vec{r})$ and AA fluctuations $\alpha(\lambda, \vec{r})$ in order to construct instantaneous polychromatic AA fluctuations with equation (6).

Optical turbulence-induced perturbations are usually obtained by inverse Fourier transforms of random complex functions of which the statistical variances are equal to the theoretical power spectra that correspond to given turbulence models [32]. The power spectrum of the monochromatic AA fluctuations we use is given by [31]

$$W_\alpha(\lambda, \vec{f}) = 0.3827 C_n^2(\lambda)\delta h f_x^2 [f^2 + L_0^{-2}]^{-11/6} \cos^2\{\pi\lambda h f^2\} \times [1 + 3.4310 f l_0 - 0.5384[f l_0]^{7/6}] \exp\left\{-\left[\frac{2\pi}{3.3} f l_0\right]^2\right\}. \quad (26)$$

The power spectrum of the monochromatic log-amplitude fluctuations is also obtained in a similar manner by

$$W_\chi(\lambda, \vec{f}) = 0.3827 \frac{C_n^2(\lambda)\delta h}{\lambda^2} [f^2 + L_0^{-2}]^{-11/6} \sin^2\{\pi\lambda h f^2\} \times [1 + 3.4310 f l_0 - 0.5384[f l_0]^{7/6}] \exp\left\{-\left[\frac{2\pi}{3.3} f l_0\right]^2\right\}. \quad (27)$$

Whenever we are concerned with spatial-like distributions of optical quantities like AA fluctuations or log-amplitude fluctuations, we can write

$$\begin{aligned} \alpha(\lambda, \vec{r}) &= \mathrm{FT}^{-1}\left\{R_1(\vec{f})\sqrt{W_\alpha(\lambda, \vec{f})}\exp\{\mathrm{i}R_2(\vec{f})\}\right\} \\ \chi(\lambda, \vec{r}) &= \mathrm{FT}^{-1}\left\{R_1(\vec{f})\sqrt{W_\chi(\lambda, \vec{f})}\exp\{\mathrm{i}R_2(\vec{f})\}\right\} \end{aligned} \quad (28)$$

where $R_1(\vec{f})$ and $R_2(\vec{f})$ are independent random numbers with respectively normal distributions with unitary variances, and uniform distributions with $0 \leqslant R_2(\vec{f}) < 2\pi$.

The Fourier transforms in equation (28) are often performed numerically with the well-known fast Fourier transform optimized procedure. This procedure imposes a regular sampling of spatial frequencies, a sampling which sometimes is not very well adapted to the spectrum shape [32]. Moreover, because the same frequencies are used for all realizations, the resulting statistical moments are those of a scale-shaped function rather than being those of a continuous power spectrum. For this reason we choose to deal with a

semi-random sampling of spatial frequencies. This sampling is homogeneous at large scale in order to ensure equilibrated presence for all frequency domains, like in the energy-cascade model [2]. Sampling is also locally randomly distributed in order to statistically ensure a complete coverage of the spectrum through many realizations. This approach is globally inspired from the random wavevectors (RWV) method [33].

Semi-random sampling is achieved by superposing small random shifts $\vec{\xi}(\vec{f}) = \xi_x(\vec{f})\vec{i} + \xi_y(\vec{f})\vec{j}$ to every frequency $\vec{f}$ of a regular sampling. If Δf denotes the grid's sampling path then $0 \leqslant \xi_x(\vec{f}) < \Delta f$ and $0 \leqslant \xi_y(\vec{f}) < \Delta f$.

The numerical integration giving rise to a given realization of the simultaneous monochromatic contributors can be summarized as follows:

$$\begin{aligned}\alpha(\lambda,\vec{r}) = {} & \frac{4\sqrt{0.3827}}{\sqrt{2}}\sqrt{C_n^2(\lambda)\delta h}\sum_{f_x,f_y>0}\Delta f R_1(\vec{f}) \\ & \times \frac{\exp\{-1.8126 l_0^2|\vec{f}+\vec{\xi}(\vec{f})|^2\}}{[|\vec{f}+\vec{\xi}(\vec{f})|^2 + L_0^{-2}]^{11/12}} \\ & \times [f_x + \xi_x]\cos\{\pi\lambda h|\vec{f}+\vec{\xi}(\vec{f})|^2\} \\ & \times \cos\{2\pi\vec{r}[\vec{f}+\vec{\xi}(\vec{f})] + R_2(\vec{f})\} \\ & \times [1 + 3.4310|\vec{f}+\vec{\xi}(\vec{f})|l_0 \\ & - 0.5384[|\vec{f}+\vec{\xi}(\vec{f})|l_0]^{7/6}]^{1/2} \qquad (29)\end{aligned}$$

$$\begin{aligned}\chi(\lambda,\vec{r}) = {} & \frac{4\sqrt{0.3827}}{\lambda\sqrt{2}}\sqrt{C_n^2(\lambda)\delta h}\sum_{f_x,f_y>0}\Delta f R_1(\vec{f}) \\ & \times \frac{\exp\{-1.8126 l_0^2|\vec{f}+\vec{\xi}(\vec{f})|^2\}}{[|\vec{f}+\vec{\xi}(\vec{f})|^2 + L_0^{-2}]^{11/12}}\sin\{\pi\lambda h|\vec{f}+\vec{\xi}(\vec{f})|^2\} \\ & \times \cos\{2\pi\vec{r}[\vec{f}+\vec{\xi}(\vec{f})] + R_2(\vec{f})\} \\ & \times [1 + 3.4310|\vec{f}+\vec{\xi}(\vec{f})|l_0 \\ & - 0.5384[|\vec{f}+\vec{\xi}(\vec{f})|l_0]^{7/6}]^{1/2}. \qquad (30)\end{aligned}$$

The constant value 4 in these equations is needed because we use one quarter of the spatial frequency plane since f_x and f_y are restricted to be positive. The other constant value $\sqrt{2}$ in the denominators is there because cosine functions are used rather than exponential functions to perform the Fourier transform. The most important constraint in the simulation is to ensure that the random quantities $R_1(\vec{f})$, $R_2(\vec{f})$ and $\vec{\xi}(\vec{f})$ are the same for all simulated quantities for every single realization.

6.2. Application to a discrete spectrum with finite bandwidth

For this simulation, we will force $\rho(\lambda)\exp\{2\chi_0(\lambda)\}$ in equation (6) to have a constant value. In this case, the expression of polychromatic AA fluctuations along a given direction is given by

$$\alpha(\vec{r}) \approx \frac{\int_{\lambda_a}^{\lambda_b} \mathrm{d}\lambda\ \exp\{2\chi(\lambda,\vec{r})\}\alpha(\lambda,\vec{r})}{\int_{\lambda_a}^{\lambda_b} \mathrm{d}\lambda\ \exp\{2\chi(\lambda,\vec{r})\}}. \qquad (31)$$

We will also consider that $C_n^2(\lambda) = C_n^2(\lambda_0)$, where λ_0 is the central wavelength.

We simulate monochromatic AA fluctuations and log-amplitude fluctuations using equations (29) and (30) with $\vec{r} = \vec{0}$. Wavelength values λ range with a regular sampling from $-\Delta\lambda_{\max}/2$ to $+\Delta\lambda_{\max}/2$, where $\Delta\lambda_{\max}$ is the maximum spectral bandwidth that we want to reach. Polychromatic AA fluctuations of various bandwidths $\Delta\lambda$ are obtained by doing the summation of more or less simultaneous monochromatic contributions around the λ_0-contribution according to equation (31). The variance is finally computed through a great number of independent polychromatic AA fluctuations samples.

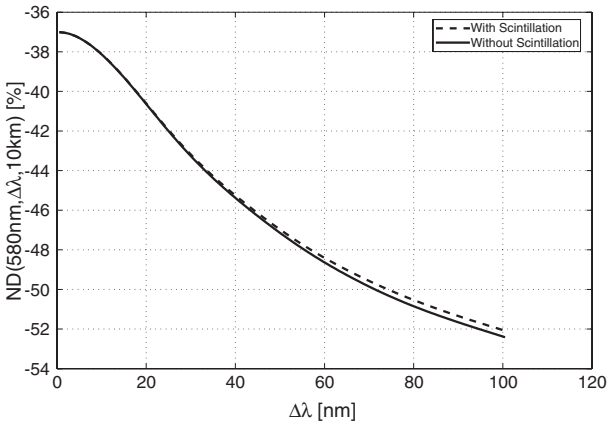


Figure 5. Plot of the 'normalized difference' (see equation (21)) on variances with respect to wavelength bandwidth as obtained with numerical simulation. In this case $L_0 = 30$ m, $l_0 = 0.01$ m, $\lambda_0 = 580$ nm, $h = 10$ km, $r_0(\lambda_0) = 0.1$ m, the number of independent realizations is $N = 2000$ and the sampling of wavelengths is $\delta\lambda = 0.25$ nm.

This simulation can easily be adapted to more realistic conditions by considering that the stellar spectrum, the detector response and optical turbulence parameters depend upon wavelength. These parameters include not only the structure constant of refractive index $C_n^2(\lambda)$ but probably both the outer scale L_0 and the inner scale l_0 of the optical turbulence too. The approximations we assume are still, however, sufficient to identify the importance or not of the phenomenon.

6.3. Results

Figure 5 presents the scintillation effects on the normalized difference defined in equation (21). It is computed versus variable wavelength bandwidth centred around λ_0 in standard turbulence conditions. The figure shows clearly that scintillation has very negligible effect on polychromatic AA fluctuations and may be ignored in the models. This small effect can be explained by looking at equation (31). If we assume that monochromatic scintillation is much more sensitive to wavelength than monochromatic AA fluctuations, the denominator of this equation will be statistically less fluctuating than the numerator and be considered as relatively constant. If log-amplitude fluctuations are very small, i.e., $\chi(\lambda,\vec{r}) \ll 1$, the intensity variation term $\exp\{2\chi(\lambda,\vec{r})\}$ can be approximated by $1 + 2\chi(\lambda,\vec{r})$. The equation expressing polychromatic AA fluctuations may be approximated with

$$\alpha(\vec{r}) \approx \int_{\lambda_a}^{\lambda_b} \mathrm{d}\lambda[\alpha(\lambda,\vec{r}) + 2\chi(\lambda,\vec{r})\alpha(\lambda,\vec{r})]. \qquad (32)$$

The variance is then given by

$$\sigma_\alpha^2 \approx \int_{\lambda_a}^{\lambda_b} \mathrm{d}\lambda_1 \int_{\lambda_a}^{\lambda_b} \mathrm{d}\lambda_2[\langle\alpha(\lambda_1,\vec{r})\alpha(\lambda_2,\vec{r})\rangle$$

$$+ 4\langle\chi(\lambda_1,\vec{r})\alpha(\lambda_1,\vec{r})\chi(\lambda_2,\vec{r})\alpha(\lambda_2,\vec{r})\rangle$$
$$+ 4\langle\chi(\lambda_1,\vec{r})\alpha(\lambda_1,\vec{r})\alpha(\lambda_2,\vec{r})\rangle]. \quad (33)$$

The first statistical term in the integral in equation (33) is that of the case where scintillation is ignored. The second and third terms in the integral are negligible compared to the first term. The reason is that log-amplitude fluctuations are more dependent on wavelength than AA fluctuations. This means that $\chi(\lambda_1,\vec{r})$ and $\chi(\lambda_2,\vec{r})$ are much more uncorrelated than $\alpha(\lambda_1,\vec{r})$ and $\alpha(\lambda_2,\vec{r})$. In addition $\chi(\lambda_1,\vec{r})$ and $\alpha(\lambda_2,\vec{r})$ are highly uncorrelated too.

These considerations may show why the simulation justifies ignoring scintillation when dealing with AA fluctuations in section 4. However, scintillation cannot be ignored in image motion through a finite aperture because there will appear terms of spatial covariance of log-amplitude fluctuations that are important and not negligible at all [27].

7. Conclusion

In discussing the validity of the near-field approximation when the AA fluctuations are observed, it has been shown that diffraction from distant turbulence layers has necessarily to be taken into account. This approximation and its consequence, the non-chromaticity of the AA fluctuations, are questioned.

We have shown how the effect of diffraction manifests itself mainly through two aspects. In the case of dealing with monochromatic light, the AA fluctuations for fixed turbulence strength are very dependent upon the height of turbulence above the ground (figure 1). It has been also noted that the variance of monochromatic AA fluctuations has a relatively weaker dependence upon wavelength. In the case of dealing with polychromatic AA fluctuations we find that the departure from the near-field approximation case is as large as the wavelength bandwidth is large. The difference is important (figure 2) and results from the combination of the altitude effect and the wavelength bandwidth. The polychromatic effect is due to the monochromatic AA fluctuations, which are uncorrelated because of diffraction.

With simulation we find that scintillation has a very weak impact (figure 5) but its effect is not negligible in image motion. Simulation has confirmed in fact the validity of the analytical model we propose, where scintillation is ignored in describing polychromatic AA fluctuations.

As a demonstrative example we have applied the model of polychromatic AA fluctuations to image motion in DIMM and estimated the systematic error in estimating Fried's parameter as a characterization of astronomical imaging quality. We have shown that when using a model that ignores diffraction, the near-field approximation being assumed, one overestimates the Fried parameter and consequently the astronomical imaging quality with respect to its real state. Seeing monitoring through AA fluctuations (or image motion) has thus to take into account both diffraction and polychromatic effects.

References

[1] Tatarskii V I 1971 *The Effects of the Turbulent Atmosphere on Wave Propagation* (*Israel Program for Scientific Translations*)
[2] Roddier F 1981 *Prog. Opt.* **19** 281–376
[3] Coulman C E 1985 *Ann. Rev. Astron. Astrophys.* **23** 19–57
[4] Roggemann M C and Welsh B M 1996 *Imaging Through Turbulence* (Boca Raton, FL: CRC Press LCC)
[5] Borgnino J 2004 *Astronomy with High Contrast Imaging (EAS Publications Series)* vol 12, pp 103–24
[6] Hickson P and Lanzetta K 2004 *Publ. Astron. Soc. Pac.* **116** 1143–52
[7] Beckers J M 1993 *Ann. Rev. Astron. Astrophys.* **31** 13–62
[8] Roddier F 1999 *Adaptive Optics in Astronomy* (Cambridge: Cambridge University Press)
[9] Aime C 2001 *Eur. J. Phys.* **22** 169–84
[10] Sarazin M and Roddier F 1990 *Astron. Astrophys.* **277** 294–300
[11] Sarazin M and Tokovinin A 2001 *Beyond Conventional Adaptive Optics (ESO Conf. Proc.) (Venice)* pp 7–10
[12] Tokovinin A 2002 *Publ. Astron. Soc. Pac.* **114** 1156–66
[13] Ziad A 2000 *Appl. Opt.* **39** 5415–25
[14] Martin F *et al* 2000 *Astron. Astrophys. Suppl.* **144** 39–44
[15] Martin H M 1987 *Publ. Astron. Soc. Pac.* **99** 1360
[16] Avila R *et al* 1997 *J. Opt. Soc. Am.* A **14** 3070–82
[17] Tokovinin A 2002 *Publ. Astron. Soc. Pac.* **114** 1156–66
[18] Andrews L C *et al* 1999 *J. Opt. Soc. Am.* A **16** 1417–29
[19] Dravins D *et al* 1997 *Publ. Astron. Soc. Pac.* **109** 173–207
[20] Sasiela R J 1994 *Electromagnetic Wave Propagation in Turbulence* (Berlin: Springer)
[21] Tavis M T and Yura H T 1987 *J. Opt. Soc. Am.* A **4** 57–9
[22] Borgnino J *et al* 1989 *J. Opt. Soc. Am.* A **6** 244–51
[23] Dravins D *et al* 1997 *Publ. Astron. Soc. Pac.* **109** 725–37
[24] Berio P *et al* 1999 *J. Opt. Soc. Am.* A **16** 872–81
[25] Voitsekhovich V V *et al* 2001 *Astron. Astrophys.* **368** 1133–6
[26] Voitsekhovich V V *et al* 2002 *Rev. Mex. Astron. Astrophís.* **38** 193–8
[27] Tokovinin A A 2003 *J. Opt. Soc. Am.* A **20** 686–9
[28] Borgnino J 1990 *Appl. Opt.* **29** 1863–5
[29] Borgnino J 1992 *Opt. Commun.* **91** 267–79
[30] Voitsekhovich V V 1995 *J. Opt. Soc. Am.* A **12** 1346–53
[31] Innocenti C and Consortini A 2004 *Proc. SPIE* **5237** 25–30
[32] Lane R G *et al* 1992 *Waves Random Media* **2** 209–24
[33] Voitsekhovich V V *et al* 1999 *Appl. Opt.* **38** 3985–92